Nonlinear Analysis of Damaged Stiffened Fuselage Shells Subjected to Combined Loads

James H. Starnes, Jr.[1], Vicki O. Britt[1], Richard D. Young[2], Charles C. Rankin[3], Charles P. Shore[1] and Nancy Jane C. Bains[1]

[1]NASA Langley Research Center
Hampton, VA

[2]Lockheed Engineering and Sciences Company
Hampton, VA

[3]Lockheed Palo Alto Research Laboratory
Palo Alto, CA

Abstract

The results of an analytical study of the nonlinear response of stiffened fuselage shells with long cracks are presented. The shells are modeled with a hierarchical modeling strategy that accounts for global and local response phenomena accurately. Results are presented for internal pressure and mechanical bending loads. The effects of crack location and orientation on shell response are described. The effects of mechanical fasteners on the response of a lap joint and the effects of elastic and elastic-plastic material properties on the buckling response of tension-loaded flat panels with cracks are also addressed.

Introduction

Transport fuselage shell structures are designed to support combined internal pressure and mechanical flight loads which can cause a geometrically nonlinear response of the shell. The structural response of a stiffened fuselage shell with one or more local cracks is influenced by the local stress and displacement gradients near the cracks and the internal loads in the shell. The response of a stiffened fuselage shell with a crack must be understood to determine the structural integrity of the fuselage and to predict its residual strength. As a crack grows in a stiffened shell, the stiffness and internal load distributions change, and these changes affect the local stress and displacement gradients near the crack in a manner that may cause additional crack growth. The structural integrity of a stiffened fuselage shell that has a crack and that is subjected to combinations of internal pressure and mechanical flight loads can be studied analytically with a nonlinear structural analysis procedure that models crack growth in the shell.

The present paper describes the results of an analytical study of the nonlinear response of stiffened fuselage shells that are subjected to combined

internal pressure and mechanical loads and that have long cracks. A hierarchical modeling strategy is used to represent the global and local response characteristics of stiffened shells with long cracks. This modeling strategy uses sufficient modeling detail to predict accurately the local stress and displacement gradients in a shell. These local gradients are caused by cracks in the shell and by structural details such as frames, stringers, failsafe straps, and joints. The STAGS (STructural Analysis of General Shells) nonlinear shell analysis code (Ref. 1) is used to predict the geometrically nonlinear response of the shells studied. The hierarchical global-local modeling strategy allows the internal load distribution and local stress and displacement gradients to be simulated accurately as the loads are increased and the crack grows.

The nonlinear analysis procedure and the modeling approach used in the present study are described herein. The analysis procedure used in the present study maintains the shell in a nonlinear equilibrium state while a crack is grown in the shell. Analytical results are presented for stiffened shells of practical interest that are subjected to combined internal pressure and mechanical bending loads. These results demonstrate the effects of combined loads on the global response of shells with longitudinal and circumferential skin cracks and on the local stress and deflection gradients near the cracks. The effects of changing crack length and other geometric parameters on nonlinear response for different loading conditions are also discussed.

Nonlinear Analysis and Modeling Procedures

A nonlinear shell analysis procedure combined with a hierarchical modeling strategy is used in the present study to analyze the nonlinear response of stiffened fuselage shells with long skin cracks and subjected to combined internal pressure and mechanical loads. The analysis procedure simulates crack growth within a shell that is in a nonlinear equilibrium state. The analysis procedure includes the capability to examine local response phenomena, such as local stress and displacement gradients, in critical areas of a fuselage where cracks may be growing. The analysis procedure accurately models frame and stringer cross-sectional distortion and rolling and predicts the nonlinear interactions that occur between individual structural elements and larger subcomponents that result from these deformations. The details of this analysis and modeling procedure are discussed subsequently.

Nonlinear Analysis Procedure

The STAGS (STructural Analysis of General Shells) nonlinear finite element analysis code (ref. 1) is used in the present study to conduct the nonlinear structural analyses of stiffened shells with long cracks. STAGS is a finite element code for analyzing general shells that includes the effects of geometric and material nonlinearities in the analysis. STAGS is capable of conducting strength, stability and collapse analyses for general shell structures. The code uses both the modified and full Newton methods for its nonlinear solution algorithms and accounts for large rotations of a shell by using a co-

rotational algorithm at the element level. STAGS has static and transient analysis capabilities that can be used to predict local instabilities and modal interactions that occur due to the addition of destabilizing mechanical loads such as an applied bending moment. The Riks arc-length projection method is used in STAGS to continue the solution past the limit points of a nonlinear response. A boundary constraint function, based on a least-squares analysis, is used in STAGS to apply equivalent beam loads to the boundary of the thin shell finite element model. By using this least-squares constraint function, flight loads can be extracted from a global aircraft structural model and then applied as edge loads on the boundaries of a refined finite element model of a fuselage shell section as shown in figure 1.

STAGS can perform crack-propagation and residual-strength analyses and can represent the effects of crack growth on nonlinear shell response. A virtual crack extension method and a load relaxation technique are used in STAGS to extend the length of a crack while the shell is in a nonlinear equilibrium state. With this method, the forces necessary to hold the nodes together along the path of new crack growth are calculated. These forces are then released and a new equilibrium state is calculated which corresponds to the additional crack growth. The changes in the stiffness matrix and internal load distribution that occur during crack growth are accounted for in the analysis, and the nonlinear coupling between internal forces and inplane and out-of-plane displacement gradients that occurs in a shell is properly represented. STAGS has an adaptive mesh refinement capability that models self-similar and non-self-similar crack-growth trajectories and can model changes in shell response due to a change in the direction of crack growth. Non-self-similar crack growth, which is determined by using an adaptive mesh refinement technique, is modeled using the crack simulation code FRANC3D (ref. 2). FRANC3D includes an automatic mesh generator that can model an arbitrary region surrounding a crack. When modeling non-self-similar crack growth, FRANC3D is used as a graphical interface between the user and STAGS. Cracks in structural elements, such as frames, stringers, and tear straps, can also be modeled by STAGS. Results from STAGS calculations include strain energy release rates and stress intensity factors which can be used to calculate the residual strength of a damaged shell.

Hierarchical Modeling Procedure

A hierarchical stiffened-shell modeling strategy is used herein for the analysis of stiffened fuselage sections as shown in figure 2. The hierarchical modeling strategy begins with a global nonlinear analysis of a large stiffened fuselage section that is subjected to combined internal pressure and mechanical loads. The mechanical loads are applied to the ends of the fuselage section and can include axial and vertical shear loads, torsion, and bending moments. The global model includes structural details such as frames, stringers, tear straps, shear clips, and floor beams. The frames, which have a nonsymmetric cross section, are modeled with beam and shell elements in order to represent accurately the cross-sectional bending of the frame. The stringers, shear clips, tear straps, and floor beams are modeled with beam elements. Damage is included in the model in the form of longitudinal or circumferential cracks and

may also include broken frames, stringers, and tear straps. Displacements and internal forces are obtained from the analysis of the global model and are then used as boundary conditions in the next level of modeling detail used in the hierarchical modeling strategy.

The second level of modeling detail used in the hierarchical modeling procedure is a stiffened-panel structural model (see figure 2). This stiffened-panel model has a higher degree of mesh refinement and structural detail than the global model previously described in order to characterize the structural response more accurately. Frames, stringers, and shear clips are modeled as branched shells in the stiffened-panel model, and the tear straps are modeled using shell elements. Distortion of structural elements, such as frames and stringers, is accounted for at this modeling level, and a mesh with sufficient refinement around the crack tip is used to calculate some crack-growth parameters.

Displacements and forces obtained from the stiffened-panel model, or second level of modeling detail, are used as boundary conditions for a third level of modeling detail that includes smaller, more-detailed local-panel models. These detailed local models include a damaged area of the shell and may also include such structural details as lap joints and fasteners which STAGS models using nonlinear springs. Finally, a fourth level of local modeling detail is used to represent accurately the shell response in the area near the crack tip. A detailed fracture mechanics analysis is performed at this modeling level to determine crack growth and propagation characteristics. As a crack grows, changes occur in the stress and displacement fields of the local models. These changes are accounted for in the more global models by reanalyzing these models with the new crack configuration. This procedure is repeated for all levels of modeling detail at each stage of crack growth.

Results and Discussion

The results of an analytical study of the nonlinear response of stiffened fuselage shells with long cracks are presented herein. Results are presented for fuselage shells subjected to internal pressure and mechanical bending loads that show the effects of crack location and orientation on shell response. Results that indicate the effects of mechanical fasteners on the response of a lap joint are also presented. In addition, results are presented that account for yielding that occurs in the crack tip region during crack growth. These results are used to demonstrate the effects of elastic and elastic-plastic material properties on the buckling and postbuckling response of tension-loaded flat panels with cracks and also to indicate the consequences of neglecting the out-of-plane deflections in a fracture mechanics analysis of a thin-walled structural element.

Shell with Internal Pressure Load

An example of the hierarchical modeling strategy described herein and the corresponding analysis results for a stiffened shell subjected to 8 psi of internal

pressure are shown in figure 3. A global fuselage model that characterizes a typical stiffened fuselage shell section is shown in the upper right of the figure. Contour plots of the hoop stress resultants in the shell are shown on the corresponding deformed shapes in the figure for all models. There is a 10-inch-long longitudinal skin crack located between two stringers and two frames in the crown of the fuselage. The crack length is extended to 20 inches using the load relaxation technique while the shell is in a nonlinear equilibrium state. Displacements obtained from the analysis of this global model for various crack lengths are applied as boundary conditions to the second level of modeling detail which is represented by the six-bay by six-bay crown-panel section model shown in the upper left part of the figure. At this level of refinement, the stress gradients are more localized in the area of the frame than for the larger, less-refined global fuselage model. Displacements obtained from the crown-panel section model are applied as boundary conditions to a two-bay by three-bay local-panel model that is centered around the crack. This third level of modeling detail is referred to in the figure as the crack extension model and has a higher level of mesh refinement than the second level of modeling detail, or the panel model, in order to represent the behavior of the crack region more accurately. The crack length is grown from 10 inches to 20 inches during the analysis using the load relaxation technique while maintaining equilibrium in the nonlinear state for both the second and third levels of modeling detail. The panels at the bottom of figure 3 represent the changes in the hoop stress and normal deflection gradients that occur as a result of crack growth.

Shell with Internal Pressure and Bending Loads

The effects of combined internal pressure and mechanical bending loads on the response of a stiffened fuselage section with a 10-inch-long longitudinal crack located in the fuselage crown are illustrated in figures 4, 5, and 6. The axial stress resultants are shown in figure 4 for three load cases: an internal pressure load; an internal pressure load plus a down-bending moment; and an internal pressure load plus an up-bending moment. An up-bending moment is defined as shown on the global shell model in figure 2. The axial stress resultants for the internal pressure load case are distributed uniformly around the circumference of the shell except where the floor beams are attached to the frames. For the case where the shell is subjected to internal pressure and a down-bending moment, the axial stress resultant contours indicate that the crown is in tension and the keel is in compression. For the case where the shell is subjected to internal pressure and an up-bending moment, the axial stress resultants in the keel are in tension and those in the crown are in compression except for the local region near the crack. The skin at the edge of the crack is in tension in the axial direction due to the bulging deformation that occurs in the local region of the crack which is caused by the internal pressure load.

Axial stress resultants for a two-bay by three-bay local model with a crack are shown in figure 5 for the three load cases shown in figure 4. The changes in the axial stress resultant fields are shown in this figure as the crack length grows from 10 to 20 inches. For the case when the fuselage crown is in compression, axial tension stress resultants exist at the edge of the crack due to the bulging of

the skin surrounding the crack. As the crack length grows to 15 and then to 20 inches, axial tension stress resultants develop in the skin bays adjacent to the skin bay with the crack due to the deformation of the stringers on each side of the crack.

The strain energy release rate G_1 that corresponds to a crack opening mode for a straight crack located at panel midbay is shown in figure 6 as a function of crack length for the three load cases. The results indicate that the strain energy release rates for combined internal pressure and axial tension stress resultants due to the down-bending moment are lower in value than the strain energy release rates for internal pressure acting alone. The results also indicate that the strain energy release rates for combined internal pressure and axial compression stress resultants due to the up-bending moment are higher in value than the strain energy release rates for internal pressure acting alone. These results suggest that the addition of an axial compression load in the area of a longitudinal crack would cause the crack to grow at a lower value of applied load than for the addition of an axial tension load. The axial compression load couples with the out-of-plane displacements at the edge of the crack to increase the magnitudes of the skin displacements near the crack.

Stiffened Panels with Different Damage Conditions

The effects of different damage locations and different types of structural element damage were studied in the present investigation at the stiffened-panel modeling level. A detailed six-bay by six-bay stiffened panel model with a 14-inch-long longitudinal skin crack is shown in figure 7. The panel is subjected to an internal pressure load and the stress resultants corresponding to an up-bending moment. A view of the concave side of the panel is shown at the bottom of the figure and indicates how the structural elements are modeled. Shell elements are used to model the frames as Z sections and the stringers as inverted hat sections. The shear clips and tear straps are also modeled with shell elements.

Contour plots of the hoop stress resultants for different crack locations are shown on the deformed shapes of the panel in figure 8 for an internal pressure load. The figures on the left side of figure 8 represent the shell as viewed from the convex side of the shell, and the figures on the right represent the shell as viewed from the concave side. The crack is centered over an undamaged circumferential tear strap that is located midway between two frames. Results for three crack locations are shown in the figure. The cracks are located at the edge of the tear strap that lies beneath a stringer, at the 1/4-bay location between the stringers, and at midbay between the stringers. The stress intensity factors K_I and K_{II} corresponding to the crack locations shown in figure 8 are shown in figure 9 as a function of crack length. The stress intensity factor K_I, which corresponds to a crack opening mode, has the highest value when the crack is located at midbay. The crack located adjacent to the edge of the stringer has the lowest value of K_I. The trends for the stress intensity factor K_{II}, that corresponds to a crack shearing mode, are opposite to the trends for the stress intensity factor K_I.

The effect of a broken tear strap on the hoop stress resultants for the panel are shown in figure 10 for the same three crack locations shown in figure 8. When the tear strap is broken and the crack lies adjacent to the edge of the stringer, the stringer rolls away from the center of the skin bay where the crack is located. However, when the crack is located at midbay, the stringer rolls toward the skin bay where the crack is located. The stress intensity factors for the panel with the broken tear strap are shown in figure 11. The trends for the stress intensity factors are the same as for the panel with the undamaged tear strap, but the values of the stress intensity factors for the panel with the broken tear strap are twice as large as those for the panel with the undamaged tear strap.

Shells with Circumferential Cracks

The effects of a circumferential crack on the response of a subscale pressurized aluminum cylindrical shell with spherical end-caps have also been studied in this investigation. Contour plots of the axial stress resultants are shown on the deformed shape of the unstiffened cylindrical shell subject to 8 psi of internal pressure in figure 12. The shell has a 14.4 inch radius and a 0.015 inch wall thickness. A 10-inch-long circumferential crack is located at the midlength of the shell. The internal pressure load causes the center of the edge of the crack to deflect outward, and causes the surface of the shell at the crack tips to deflect inward. This response is due to a nonlinear effect associated with the curvature of the shell. Contour plots of the axial stress resultants for a stiffened aluminum cylinder subject to 8 psi of internal pressure are shown on the shell deformed shape in figure 13. The stiffened shell has the same radius and thickness as the unstiffened shell and has rings and longitudinal stringers and a 10-inch-long circumferential crack at shell midlength. The results indicate that the stringers do not restrain the inward bending of the shell at the crack tip.

Panel with a Lap Joint

The effects of discrete fasteners on the response of a cylindrical panel with a lap joint have been studied in the present investigation using the local panel model shown in figure 14. The model represents a lap joint in one half of a single skin bay between the frames and stringers of a typical fuselage shell. The model consists of two skin elements and an inverted hat stringer at the lap joint. The elements of the joint are connected by three rows of fasteners in a staggered pattern. An expanded view of the model shows the elements or layers of the lap joint and is used to display the results for each joint element. The panel is loaded by internal pressure, and symmetry conditions and displacement constraints are applied to simulate the effects of the adjacent structure which is not modeled. The left edge of the model is clamped to simulate the influence of a frame. The right edge of the model is midway between two frames and is constrained by enforcing symmetry conditions. A comparison of the undeformed and deformed cross sections of the panel is also shown in figure 14. The local bending of the skin and stringer, and the rolling and distortion of the stringer cross section that occurs in the lap joint are indicated in the figure. These stringer cross-sectional

deformations would not be represented in a model using a conventional discrete beam model for the stringer.

Contour plots of the surface hoop strains for each skin element of the joint are shown in figure 15. Results are shown for two types of joint connections. The skin elements in the model on the right are continuously attached along the length of the joint in a manner that is similar to an adhesively bonded joint. The model on the left has discrete fasteners connecting the skin elements to form the joint. The outer-surface hoop strains of the joint skin elements are shown in figure 15a as viewed from the convex side of the shell. The view of each model is rotated in figure 15b to show the inner-surface hoop strains of the joint skin elements as viewed from the concave side of the shell. For both types of joint connections, the maximum surface hoop strain occurs on the inner surface of the outer skin element near the edge of the attachment between the inner and outer skin elements. The hoop tension loads and the eccentricity of the inner and outer skin elements couple to cause local bending in the joint which adds to the skin bending associated with the internal pressure load. For the model with the continuous attachment, this bending occurs in a region visible from the inner or concave surface of the joint. The discrete fasteners cause maximum bending to occur adjacent to the top row of fasteners, which is in a region hidden from view by the inner skin element. This location on the inner surface of the outer skin element at the top row of fasteners has been identified as a critical crack initiation site for lap joints. Crack initiation often occurs at this location because the fasteners are often countersunk into the outer skin element.

The model with the discrete fasteners was modified to study the effect of a skin crack at this critical crack-initiation site by introducing a 3-inch-long half crack along the top row of fasteners. Contour plots of the stress resultants for the undamaged panel and the panel with the 3-inch-long half crack are shown on the deformed shapes of the panels in figures 16 and 17. The hoop and axial stress resultant contours shown in figure 16 demonstrate the effects that introducing the crack have on the stress distribution, on the stress concentration at the crack tip, and on the bending of the stringer. The transverse shear stress resultant contours shown in figure 17 indicate the presence of the fastener pull-through forces at the fastener locations. Deformed shapes of three cross sections of the panel with the 3-inch-long half crack are shown in figure 18. One cross section is located ahead of the crack, one is located at the crack tip, and one is located at crack mid length. These deformed shapes demonstrate the stringer rolling and cross-section distortion that occur as a result of the deformations in the region of the crack.

Tension-Loaded Panel with a Crack

A tension-loaded flat panel with a central transverse crack was modeled as shown in figure 19 to study the effect of the transverse compression stresses on panel buckling near the crack. These transverse compression stresses are induced by the Poisson effect that occurs in plates and shells. When these compression stresses reach a critical value for a given crack length, the panel buckles into a local mode that extends above and below the crack. The mode

has one half-wave in the longitudinal and transverse directions. The finite element discretization of the panel used for the nonlinear analysis is shown in figure 19. The panel is 24 inches long, 12 inches wide, and 0.090 inch thick. The crack lengths considered are 4, 5 and 6 inches. The material is 2024-T3 aluminum alloy. The finite element model shown in figure 19 models only one half of the plate and uses 5-node transition elements for mesh refinement.

Nonlinear static analyses were conducted for each crack length using either elastic or elastic-plastic material properties. The results of these analyses are shown in figures 20 and 21. Nonlinear solutions were obtained in the prebuckling and postbuckling load range for each crack length. The shape of the first buckling mode was used as a geometric imperfection in the analysis to continue the solution onto the initial postbuckling branch of the solution. The out-of-plane displacement at the center of the crack is shown as a function of the applied tension load in figure 20 for each crack length. The results obtained using elastic material properties are shown by the solid lines, and results obtained with elastic-plastic material properties are shown by the dashed lines. The panel with the 4-inch-long crack has the highest buckling load and has the greatest reduction in buckling load and postbuckling stiffness when elastic-plastic material properties are included in the analysis. The panel with the 6-inch-long crack buckles at a substantially lower value of applied tension load than the corresponding panels with the other two crack lengths, and its buckling load and initial postbuckling response are not significantly affected by elastic-plastic behavior.

The results presented in figure 20 indicate that the buckling load is dramatically affected by the length of the crack. The buckling load is influenced by the increase in local panel flexibility near the crack as the crack length increases. The results also indicate that the stress level in the panel at the onset of buckling is higher for the shorter crack lengths than for the longer crack lengths since the buckling load increases as crack length decreases. These results suggest that buckling of the panels with the shorter crack lengths occurs at general stress levels that are high enough to yield the panel locally. The local bending stresses associated with the buckling response also add to the general stress level in the panel and can cause enough reduction in stiffness due to yielding to reduce the magnitude of the postbuckling loads to values below the elastic response curves as shown in figure 20.

Contour plots of the axial stress and strain results for the panels with 4- and 6-inch-long cracks are shown in figure 21. Results are shown for tension loads that are 20 percent greater than the buckling loads of the corresponding panels with elastic material properties. The applied tension load that is 20 percent greater than the buckling load for the panel with the 4-inch-long crack is 35,000 lbs. The axial stress resultants from the analysis with elastic material properties are significantly different from those obtained from the analysis with elastic-plastic material properties because a relatively large area of material near the crack tip has yielded. In contrast, the applied tension load that is 20 percent greater than the buckling load for the panel with the 6-inch-long crack is only 13,500 lbs. The axial stress resultants for the panel with the 6-inch-long crack

are much lower in value than the corresponding results for the panel with the 4-inch-long crack, and are essentially not affected by including elastic-plastic material properties in the analysis. In addition, the size of the area of material at the crack tip that exhibits inelastic strain is much smaller than that for the panel with the 4-inch-long crack.

Concluding Remarks

The results of an analytical study of the effects of long cracks on the nonlinear response of stiffened fuselage shells subjected to combined internal pressure and mechanical loads are presented. The results suggest that nonlinear stiffened-shell analyses provide accurate predictions of the global and local responses of stiffened shells that have cracks and are subjected to combined loads. The results of nonlinear analyses show that the response of a damaged stiffened shell subjected to combined internal pressure and mechanical loads is different from the response of the shell subjected to an internal pressure load acting alone. Structural details and built-up structures with fasteners are included in the nonlinear analyses to provide an accurate representation of practical stiffened-shell structures. In addition, crack growth is predicted in a stiffened shell while the shell is in a nonlinear equilibrium state. Large local stress and out-of-plane deflection gradients that exist near cracks in stiffened shells are predicted accurately with a nonlinear stiffened-shell analysis. The results of the analysis indicate that curvature may affect the response of a shell with a circumferential crack more than it affects the response of a shell with a longitudinal crack. It is shown that both geometric and material nonlinear effects can be important for accurately predicting crack growth in stiffened shells. As an example of the importance of these nonlinear effects, the buckling load of a tension-loaded panel with a transverse crack was found to depend on the length of the crack. The results indicate that, if the crack is short enough for the panel to have a relatively high buckling load, the stresses in a tension-loaded panel with a transverse crack can be high enough to yield the panel near the crack tip.

References

1. Almroth, B. O.; and Brogan, F. A.: The STAGS Computer Code. NASA CR-2950, 1980.

2. Potyondy, David O.: A Software Framework for Simulating Curvilinear Crack Growth in Pressurized Thin Shells. School of Civil and Environmental Engineering Report 93-5, Cornell University, August 1993.

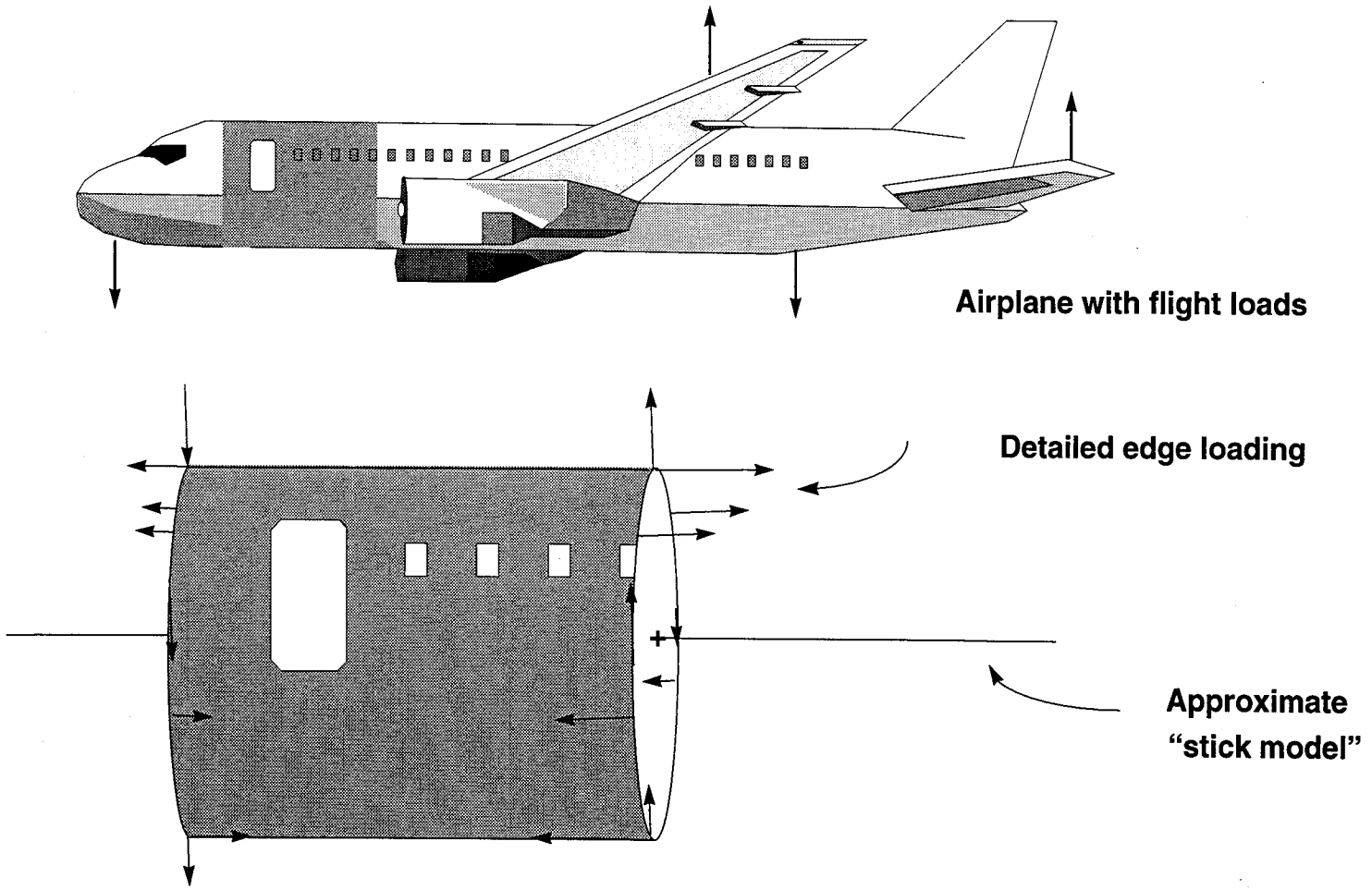

Fig. 1 Flight loads transformed to fuselage shell loads.

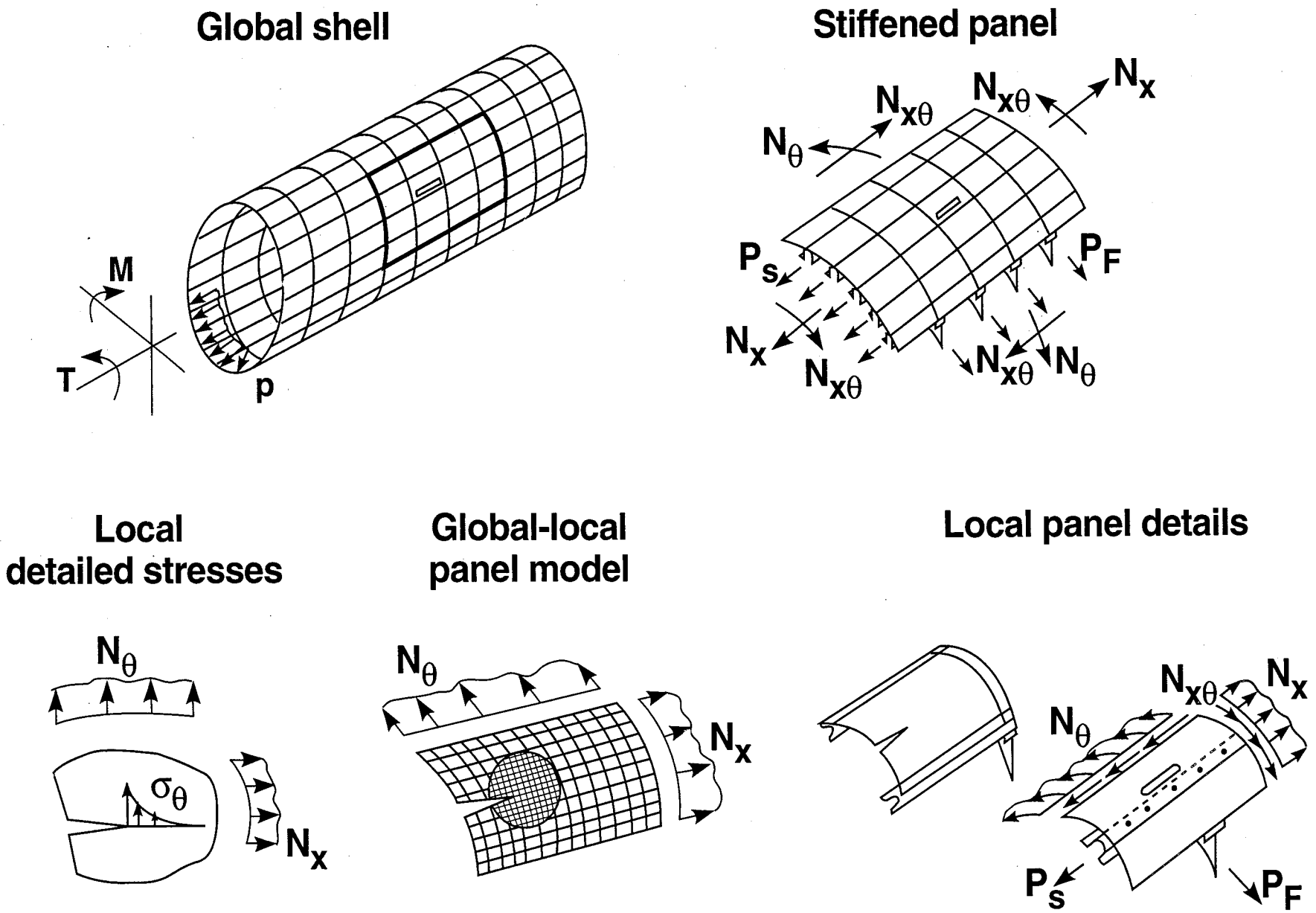

Fig. 2 Hierarchical nonlinear stiffened-shell models.

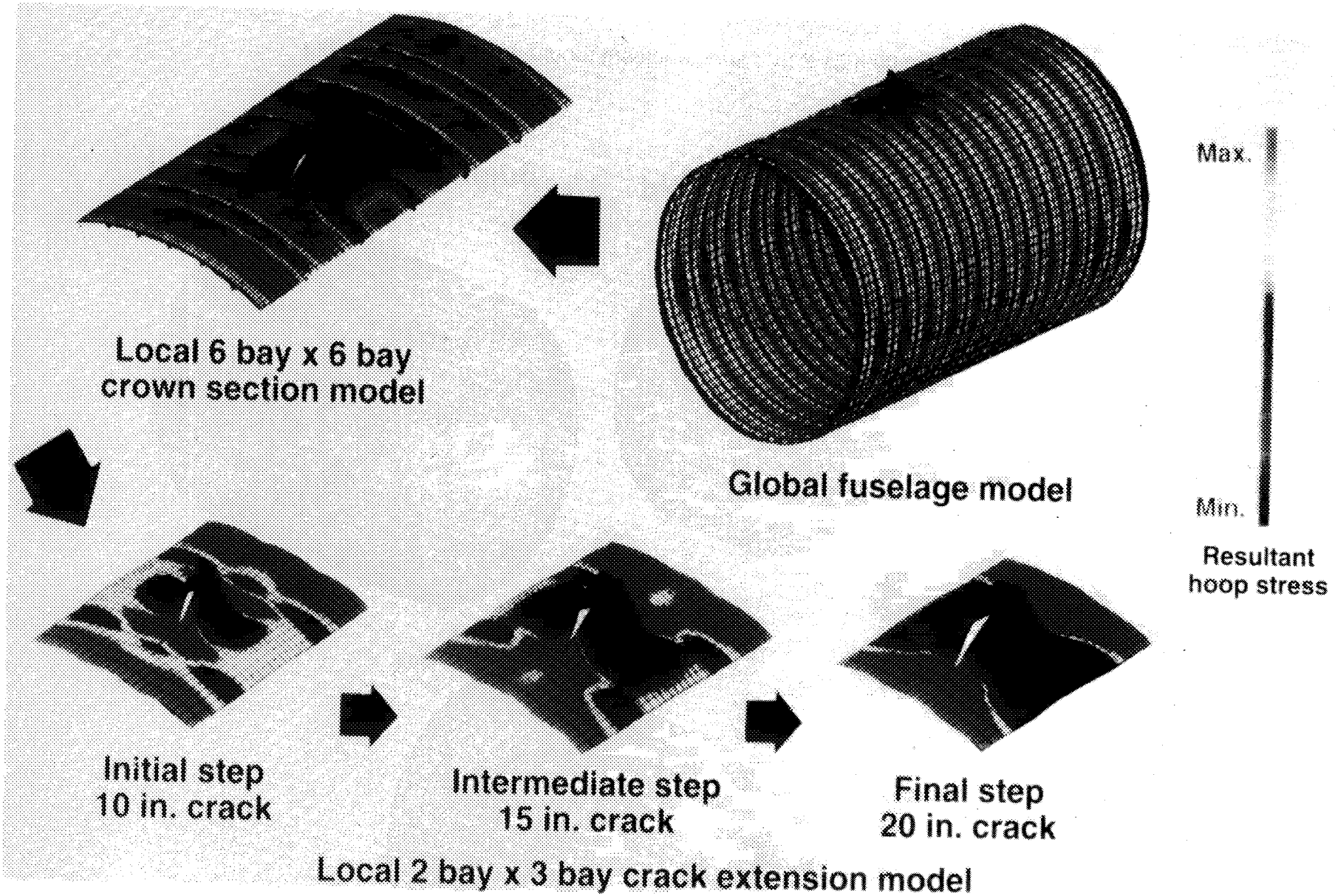

Fig. 3 Nonlinear crack growth in an aircraft fuselage structure using a hierarchical modeling strategy.

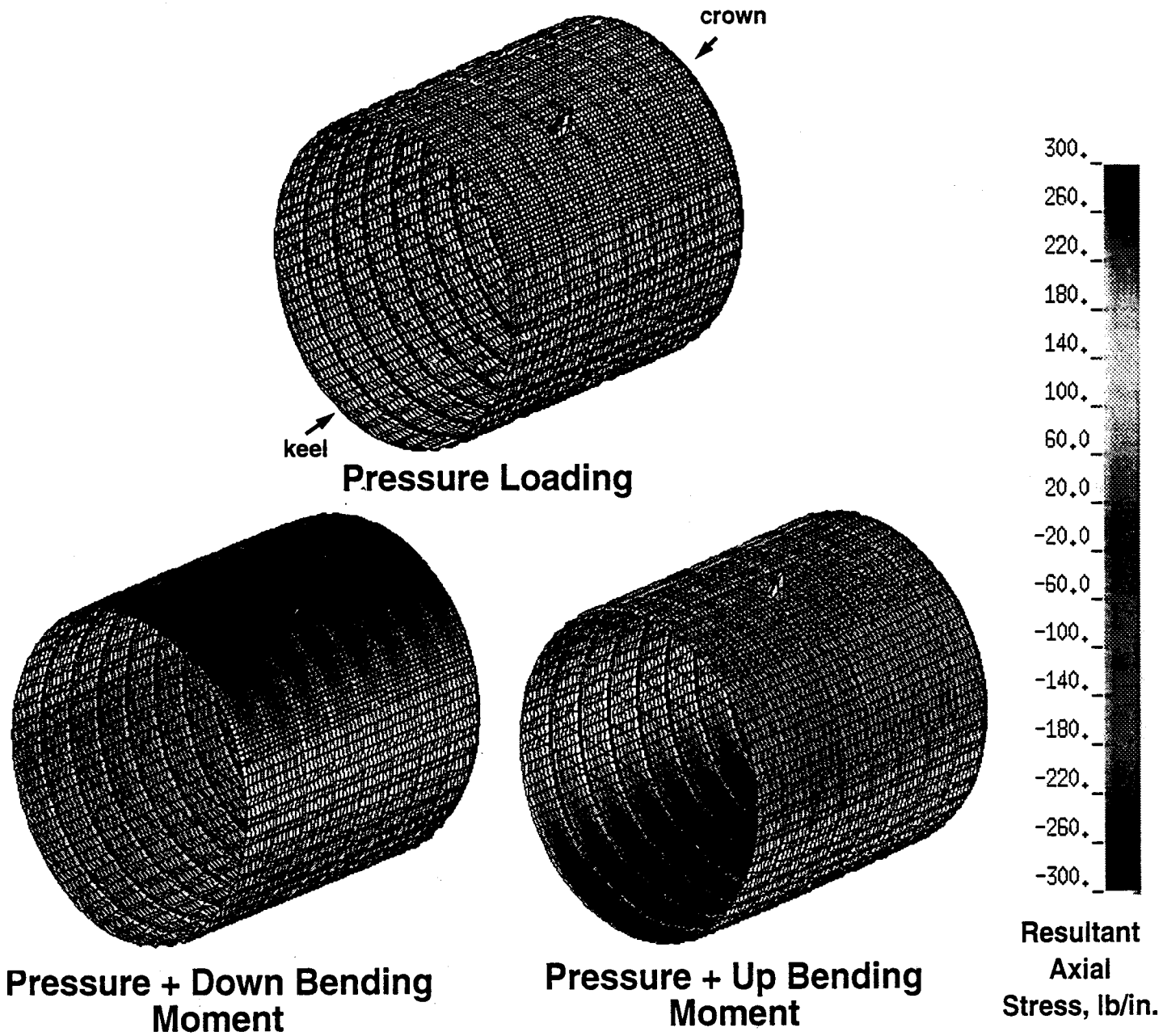

Fig. 4 Stiffened aluminum fuselage shell with a 10-inch-long skin crack.

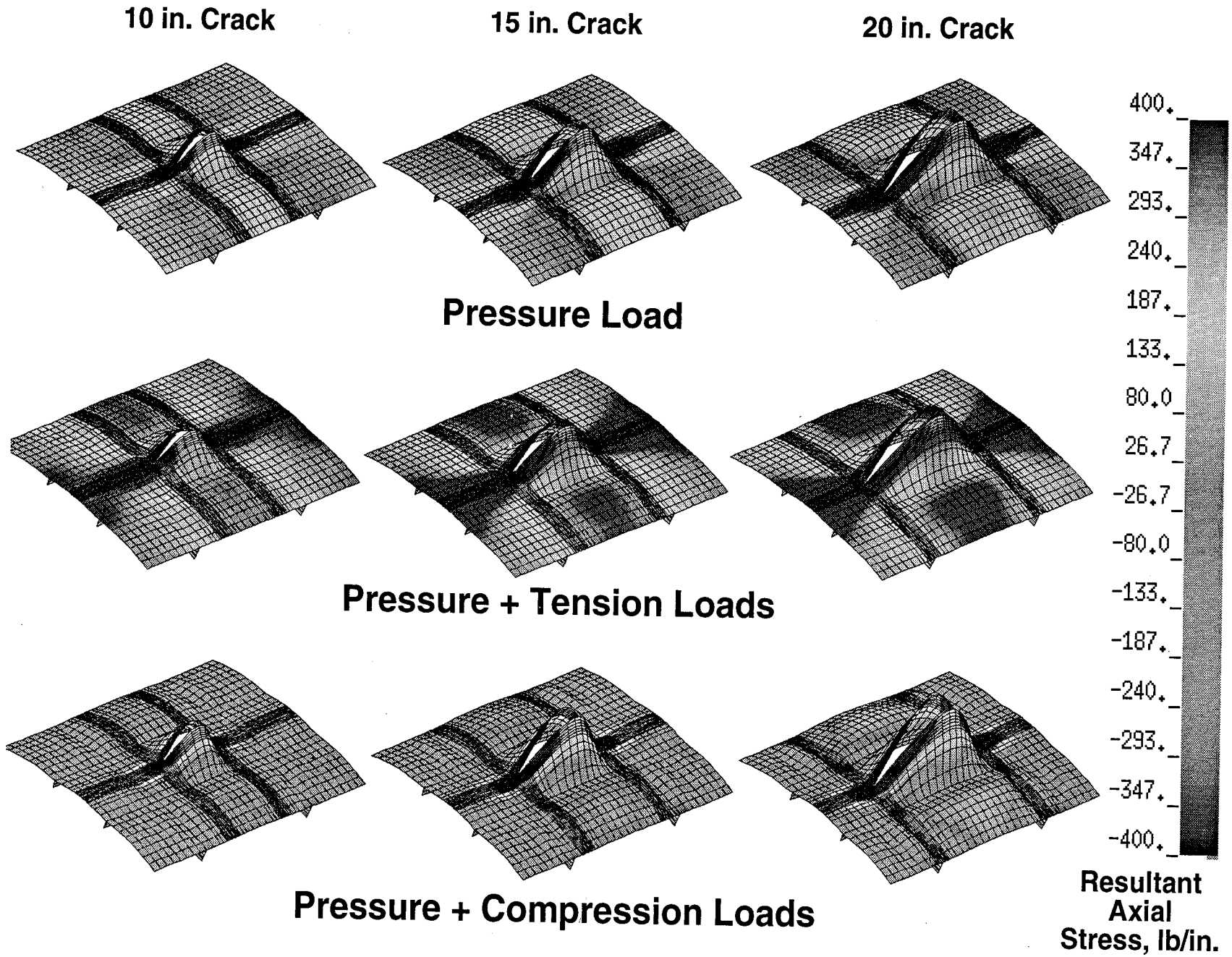

Fig. 5 Two-bay by three-bay stiffened aluminum fuselage panel model with a skin crack.

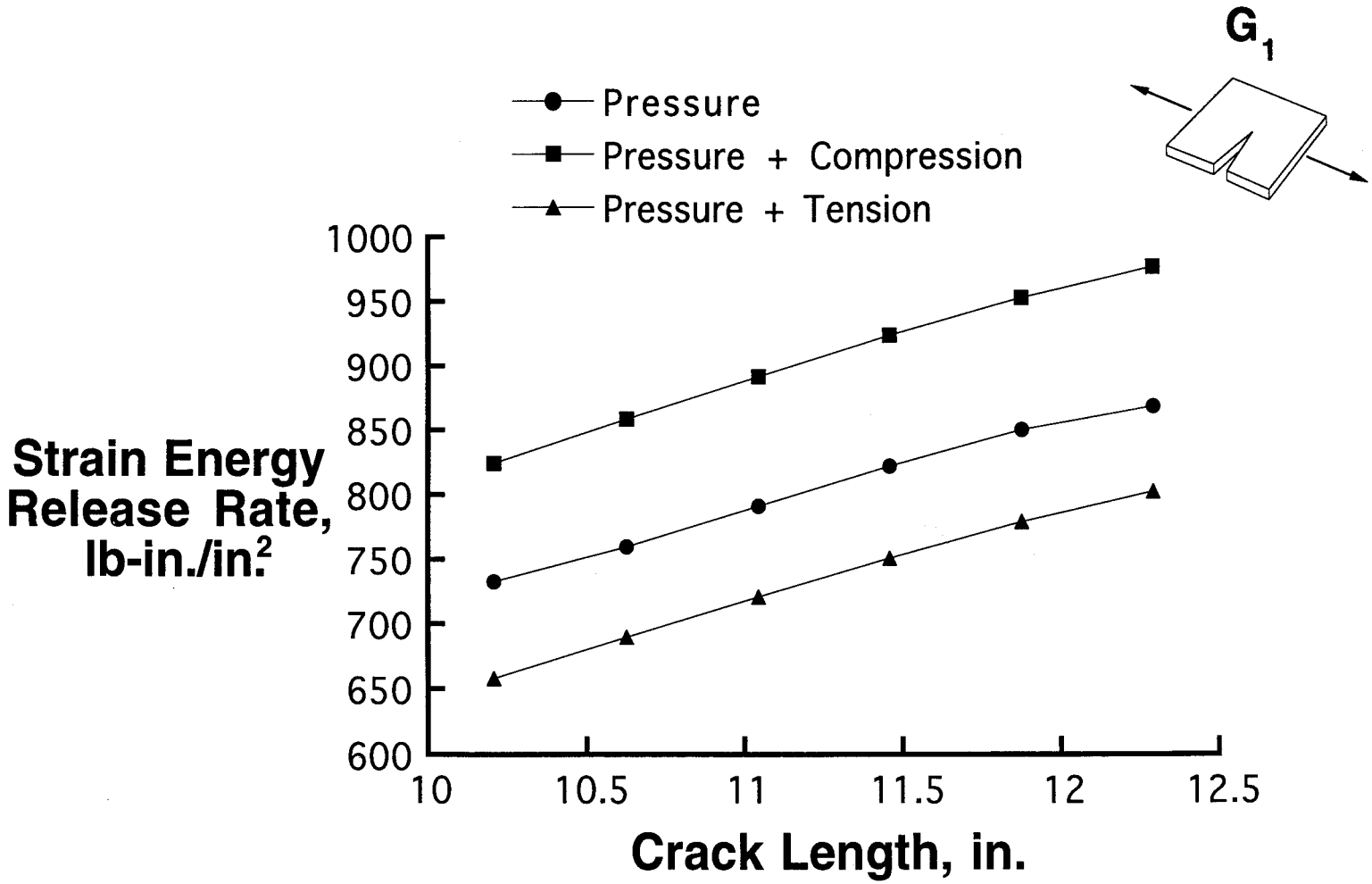

Fig. 6 Strain energy release rate for a two-bay by three-bay stiffened aluminum fuselage panel model with a skin crack.

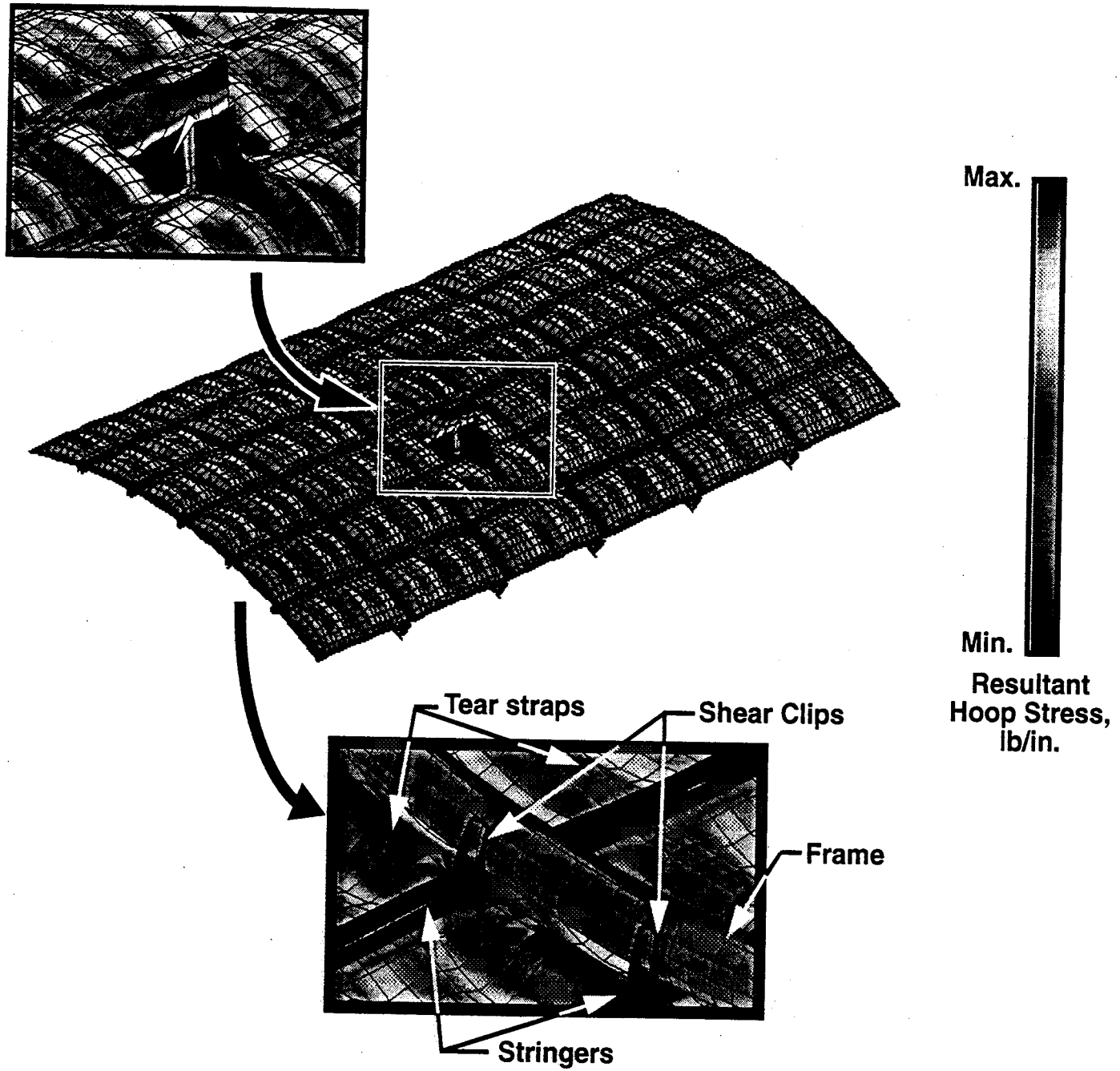

Fig. 7 Structural details of a local six-bay by six-bay stiffened-panel model subjected to internal pressure and an up-bending moment.

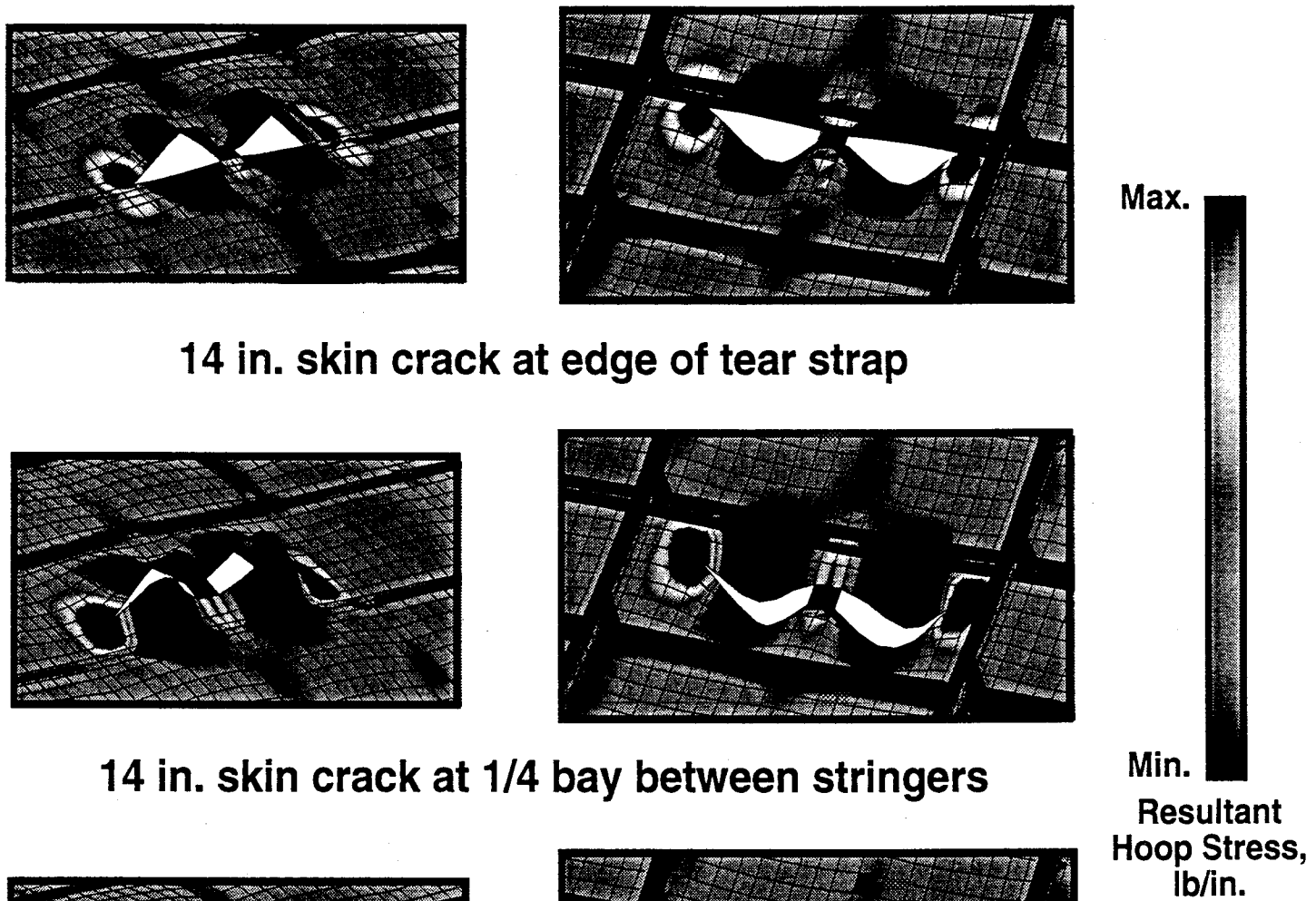

Fig. 8 Six-bay by six-bay stiffened panel with a skin crack and subject to internal pressure.

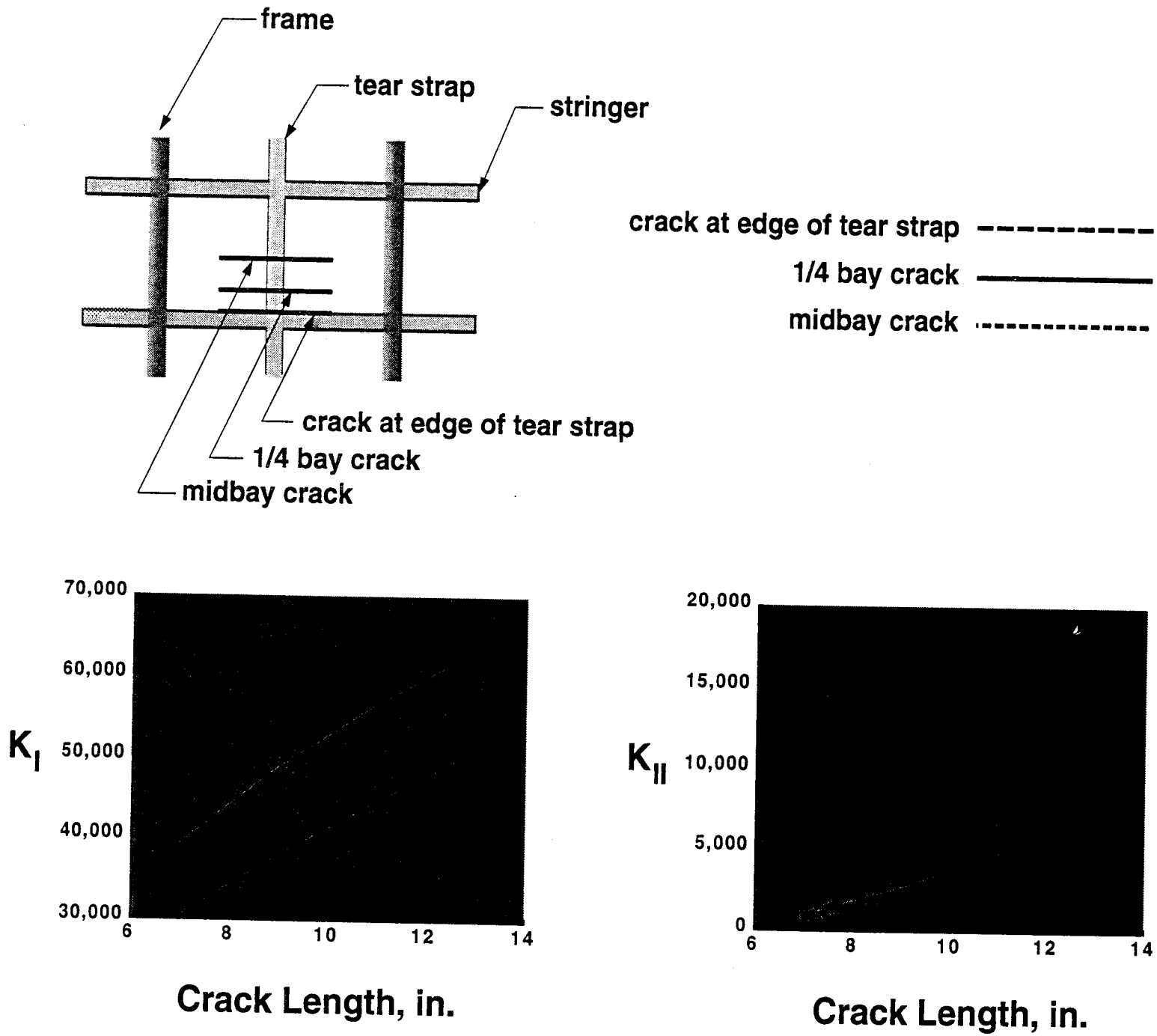

Fig. 9 Stress intensity factors for a six-bay by six-bay stiffened panel with a skin crack and subject to internal pressure.

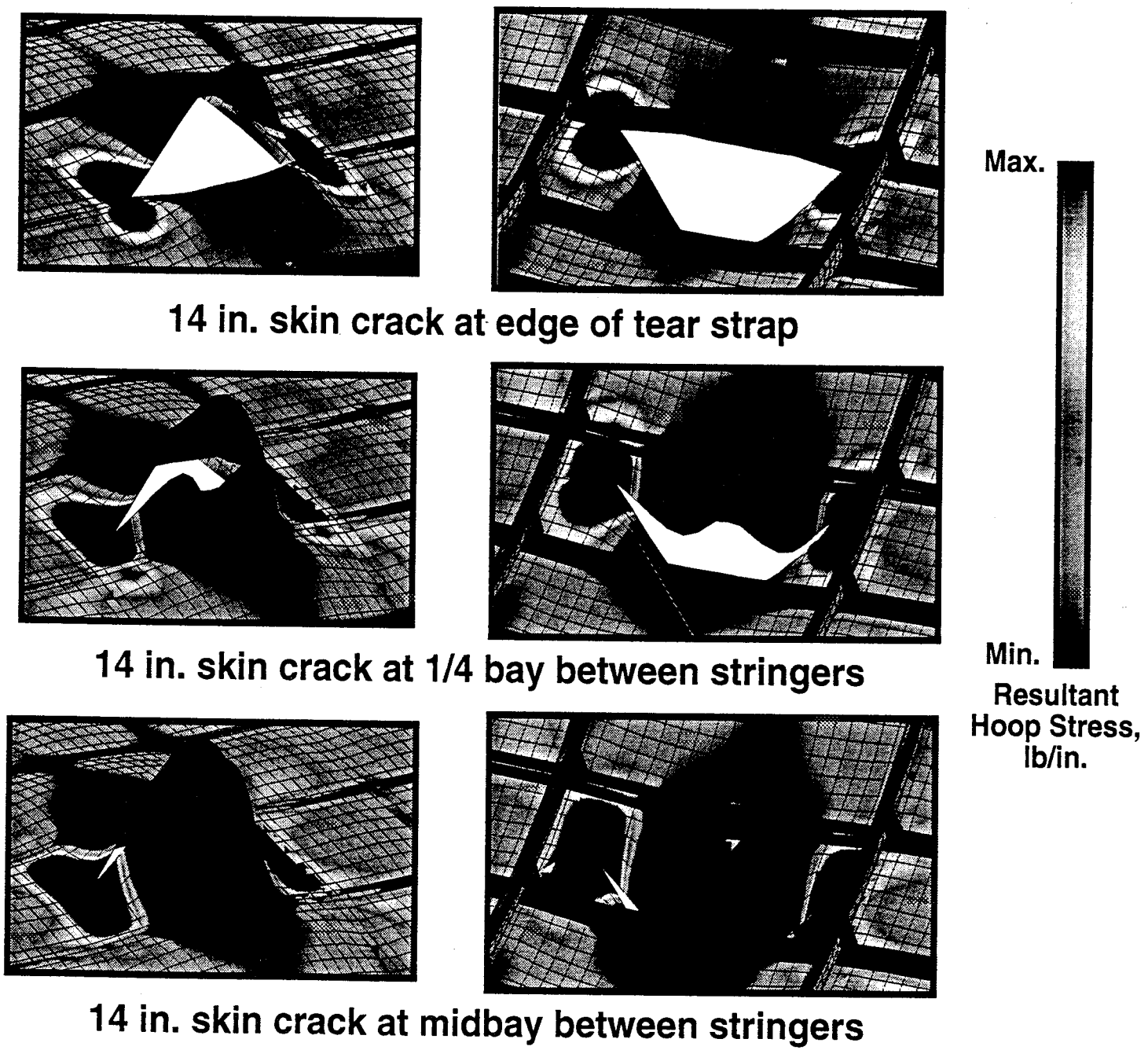

Fig. 10 Six-bay by six-bay stiffened panel with a skin crack and broken tear strap and subject to internal pressure.

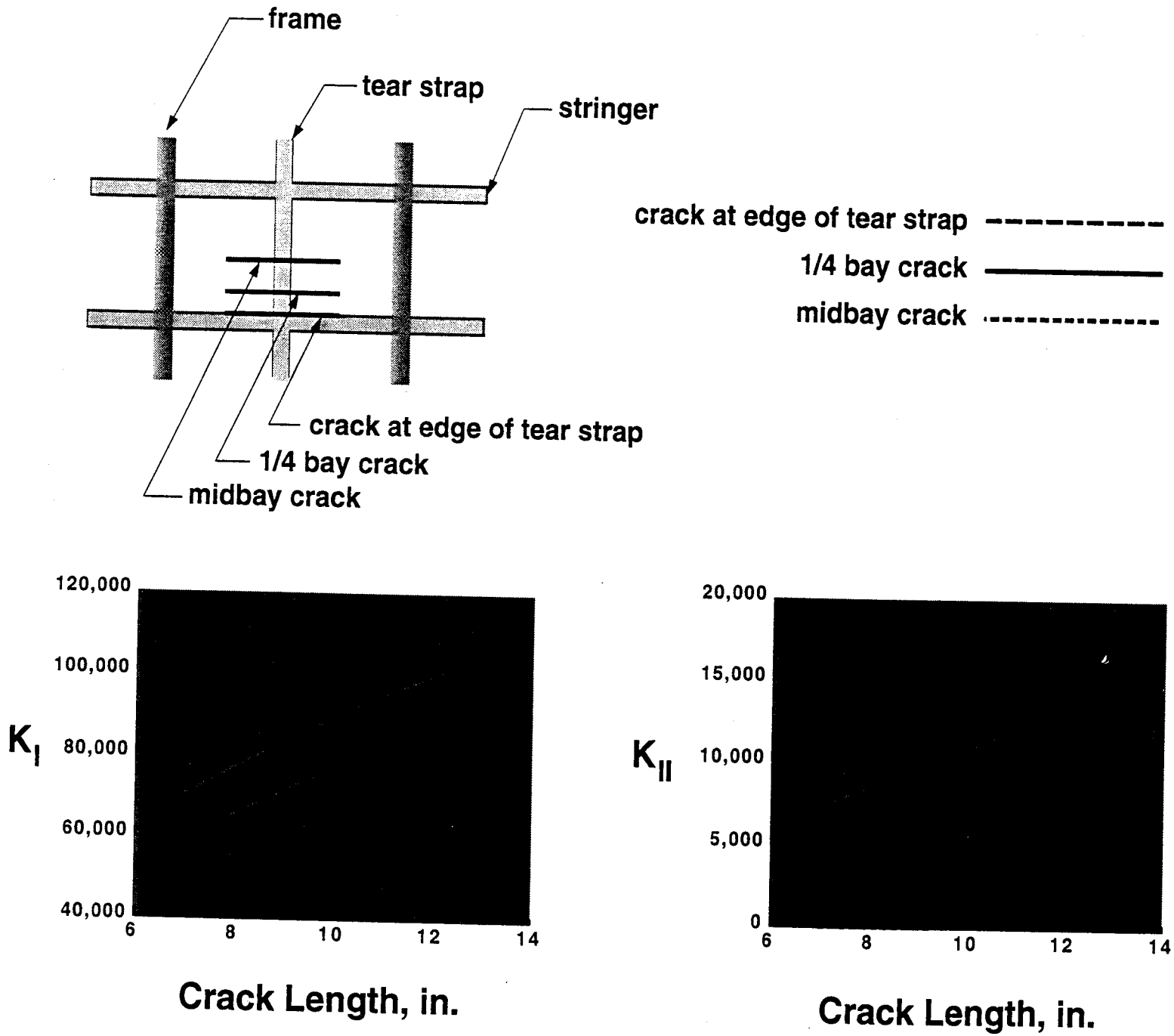

Fig. 11 Stress intensity factors for a six-bay by six-bay stiffened panel with a skin crack and a broken tear strap and subject to internal pressure.

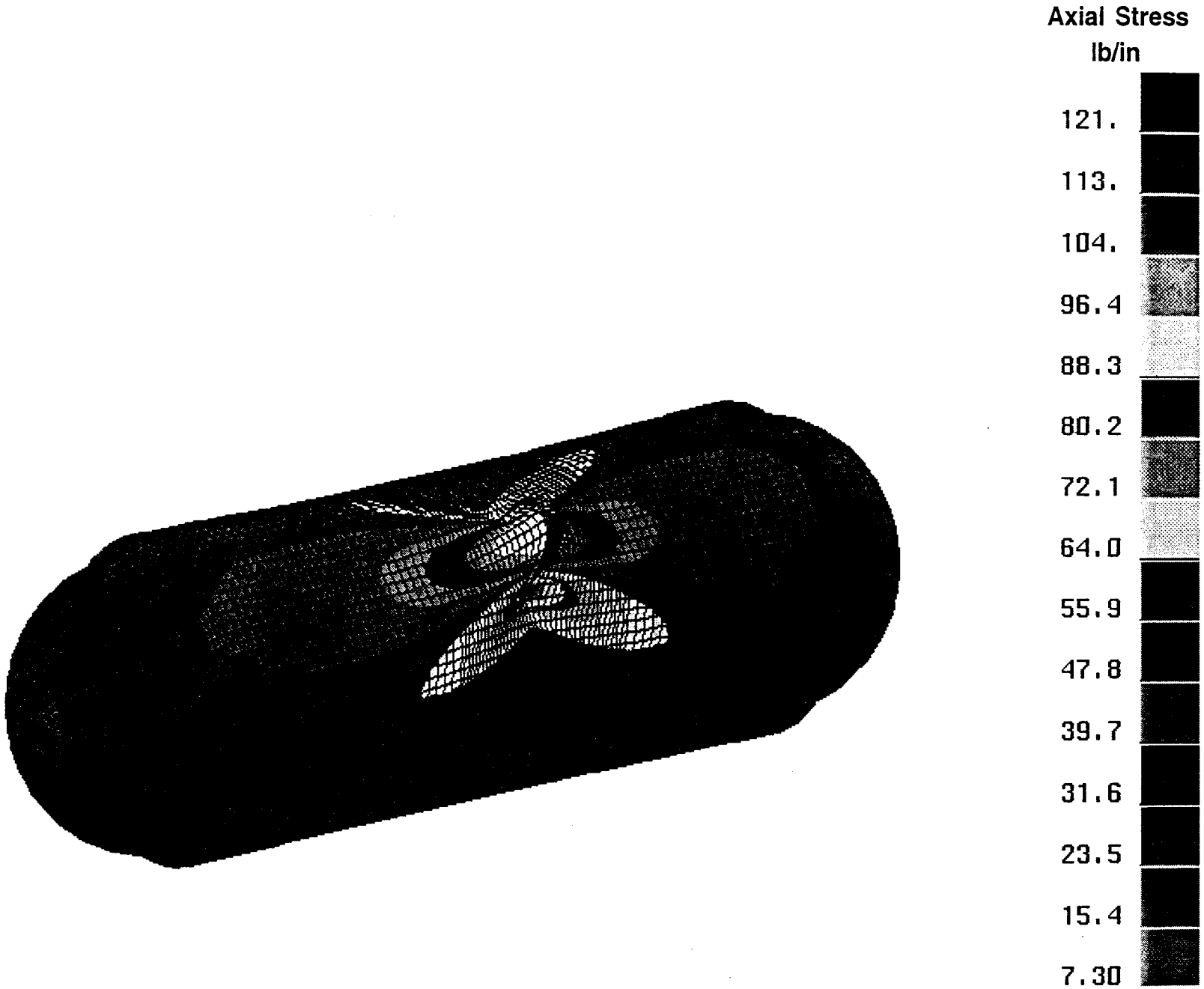

Fig. 12 Effect of a circumferential crack on the axial stress resultant distribution in a pressurized unstiffened aluminum shell.

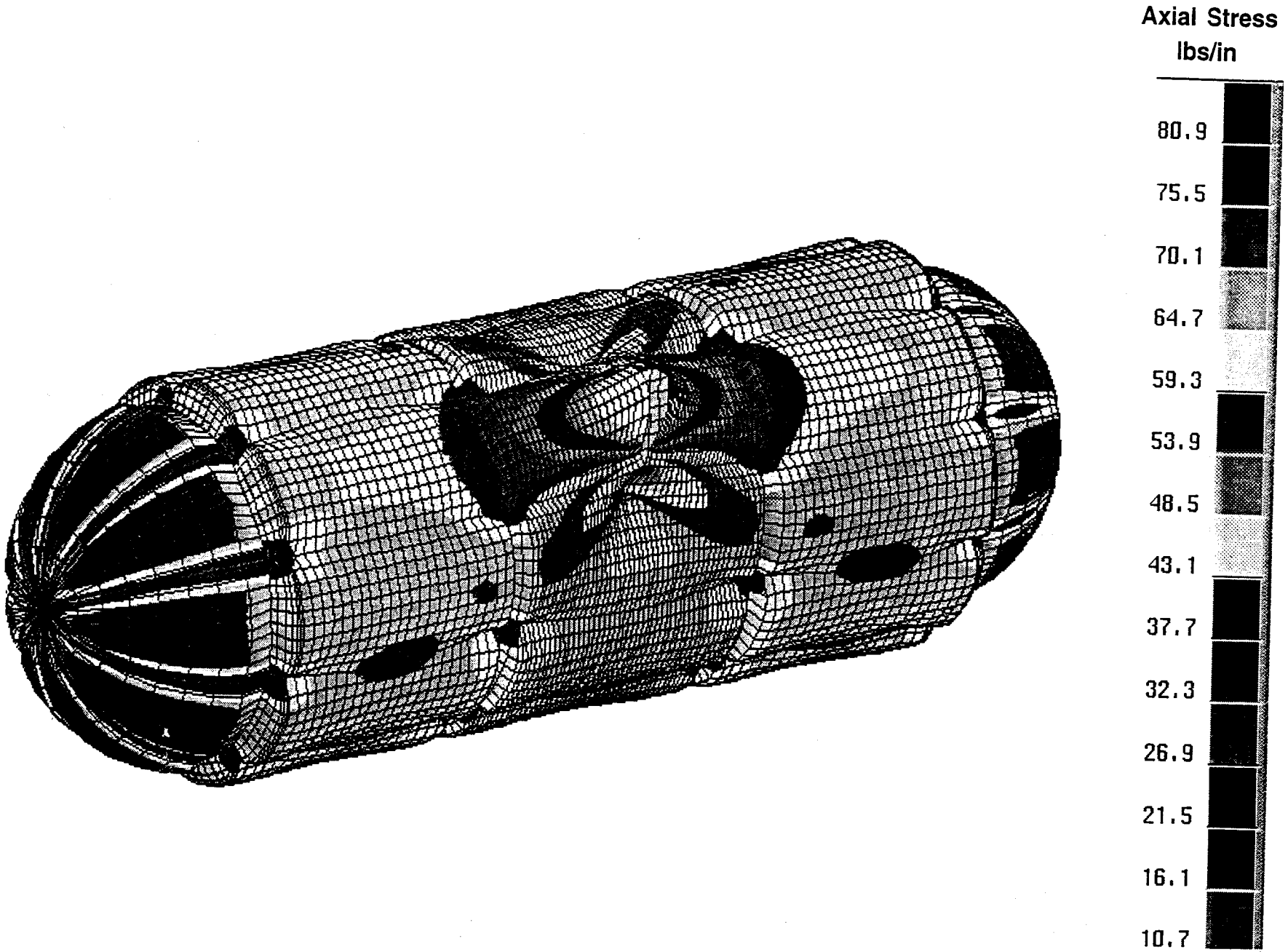

Fig. 13 Effect of a circumferential crack on the axial stress resultant distribution in a pressurized stiffened aluminum shell.

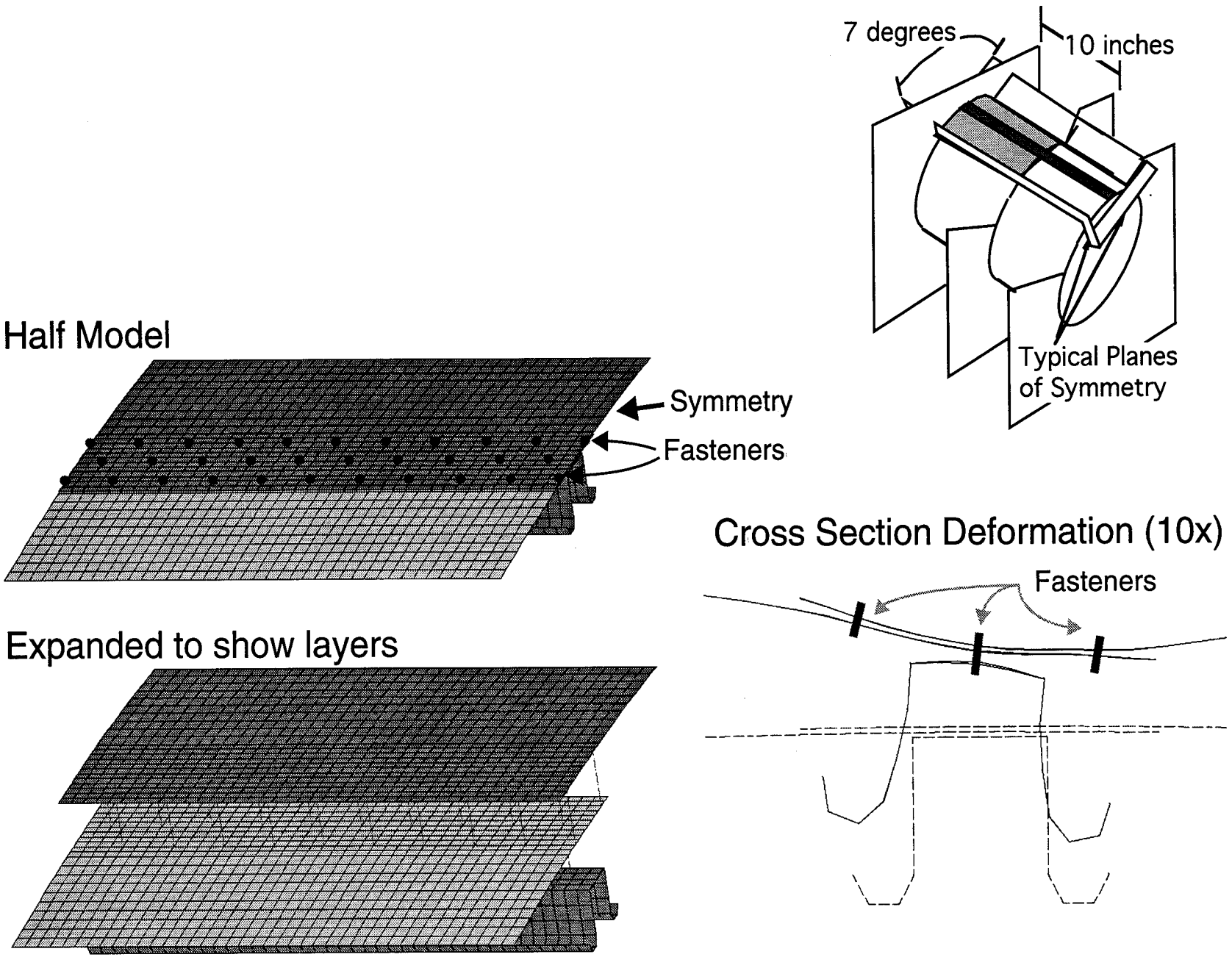

Fig. 14 Stiffened aluminum lap joint with discrete fasteners.

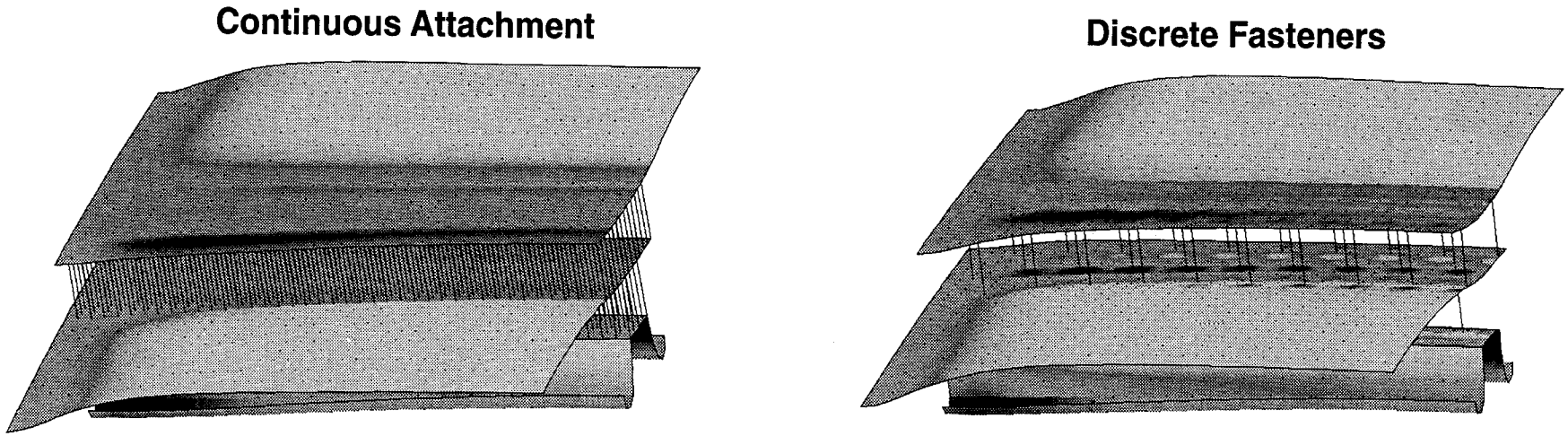

(a) Outside surface

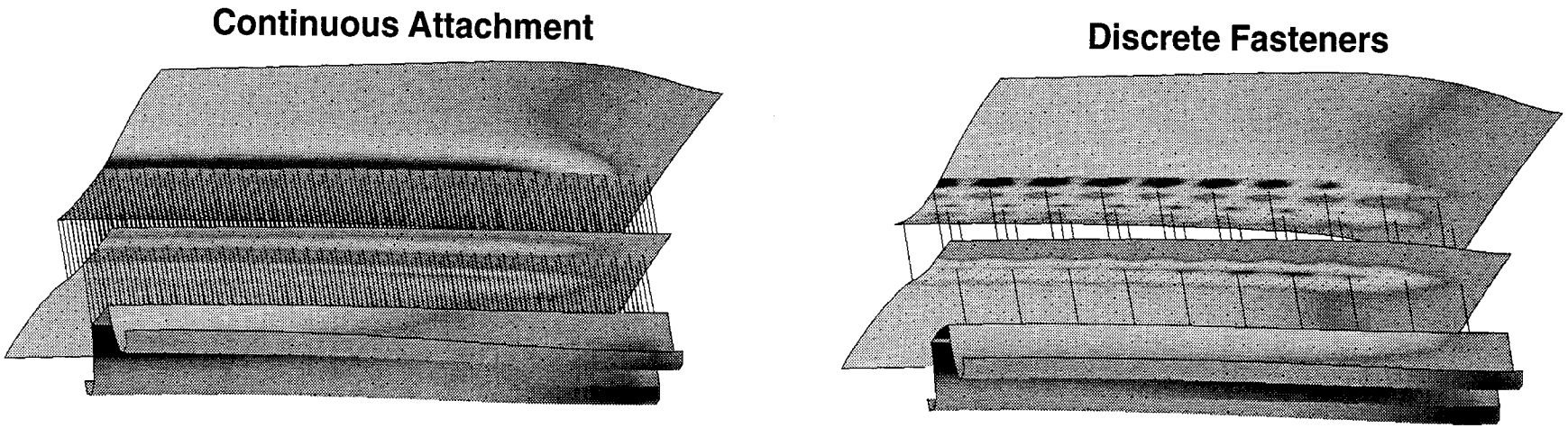

(b) Inside surface

Max. surface strain: inside surface of outer skin near top row of fasteners

Fig. 15 Surface hoop strains in lap joints that are continuously attached and have discrete fasteners.

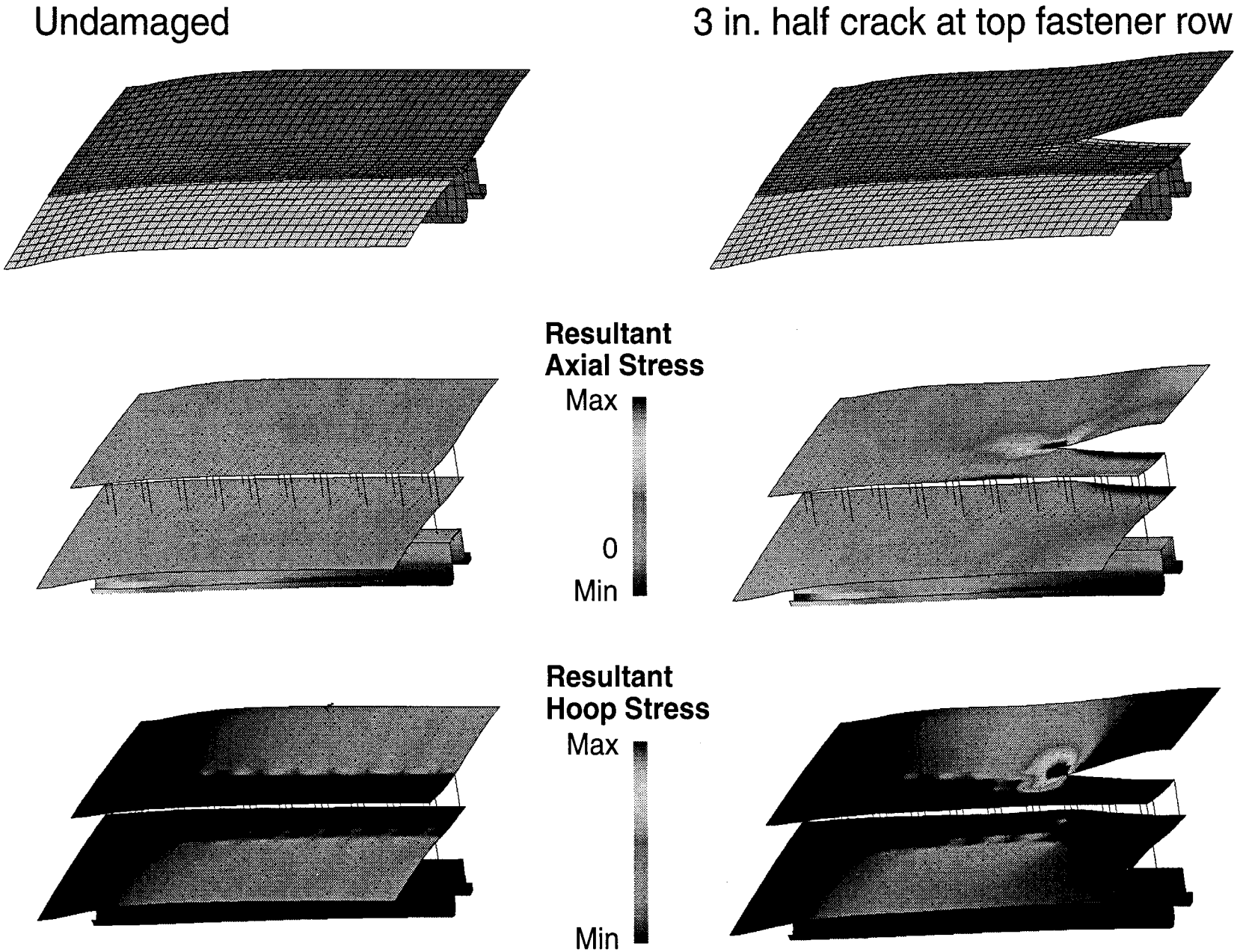

Fig. 16 Deformed shape, and axial and hoop stress resultants for an undamaged lap joint and a lap joint with a 3-inch-long half crack along the top fastener row.

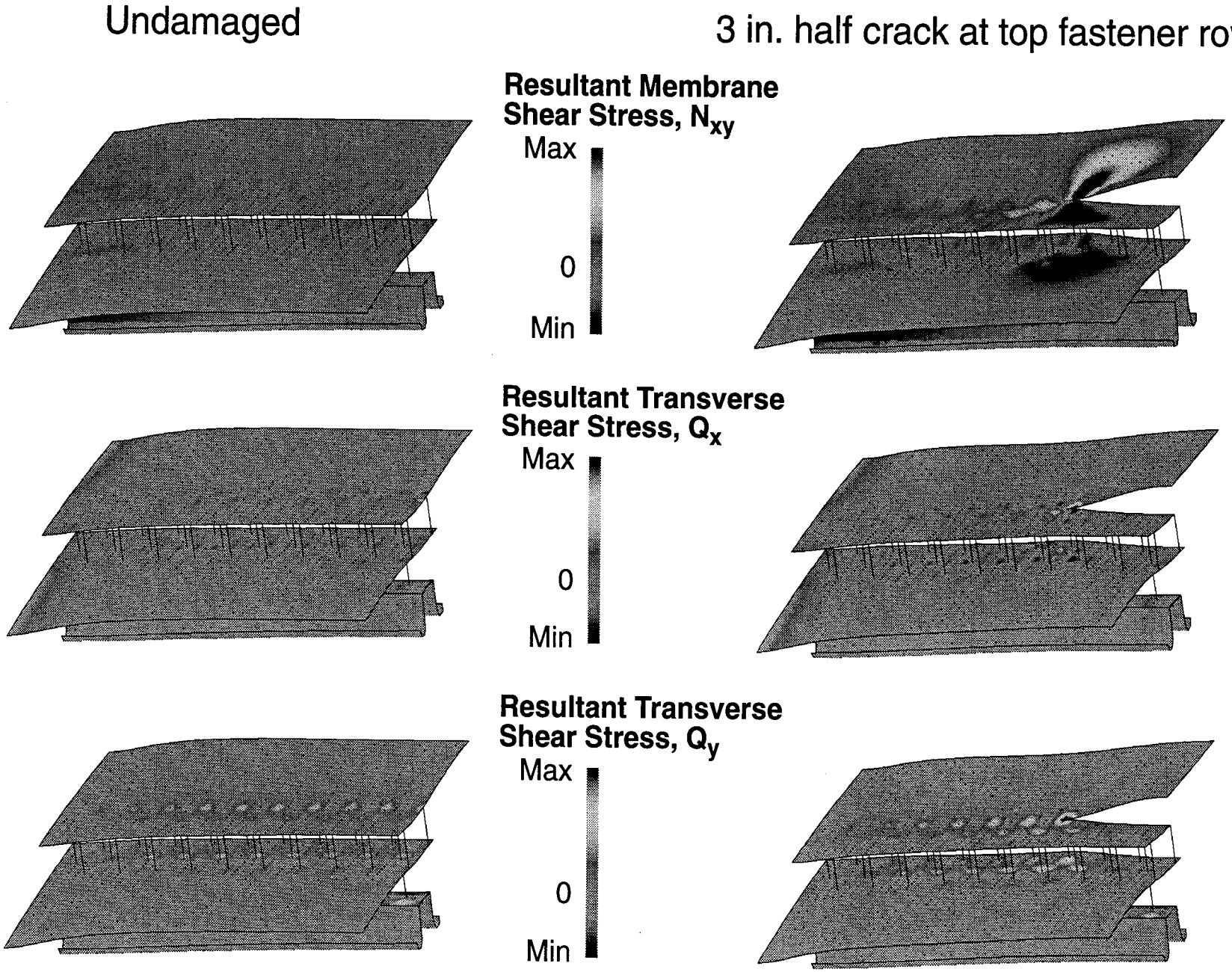

Fig. 17 Inplane and transverse shear stress resultants for an undamaged lap joint and a lap joint with a 3-inch-long half crack along the top fastener row.

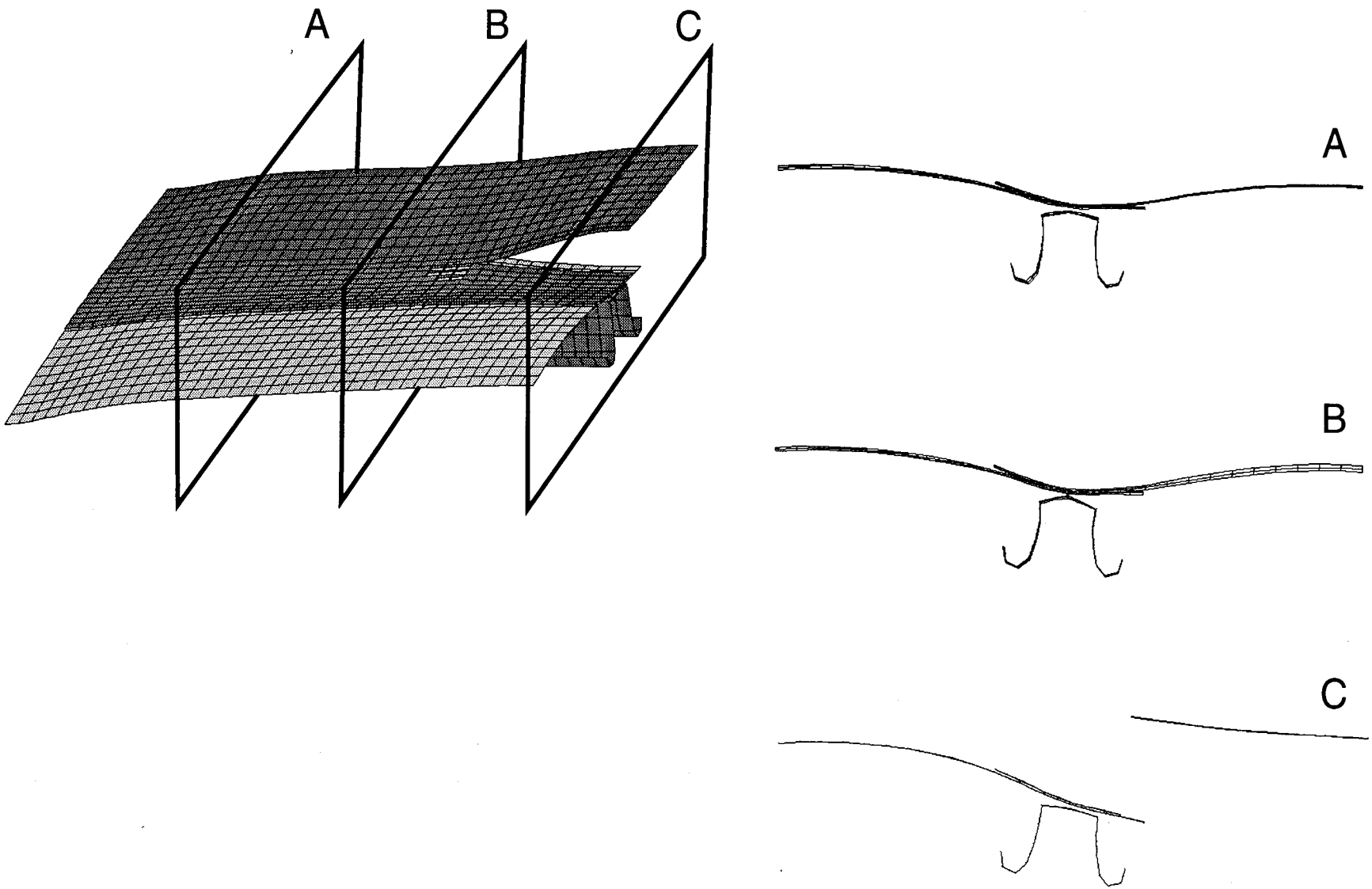

Fig. 18 Stiffener cross-section deformations for a lap joint with a 3-inch-long half crack along the top fastener row.

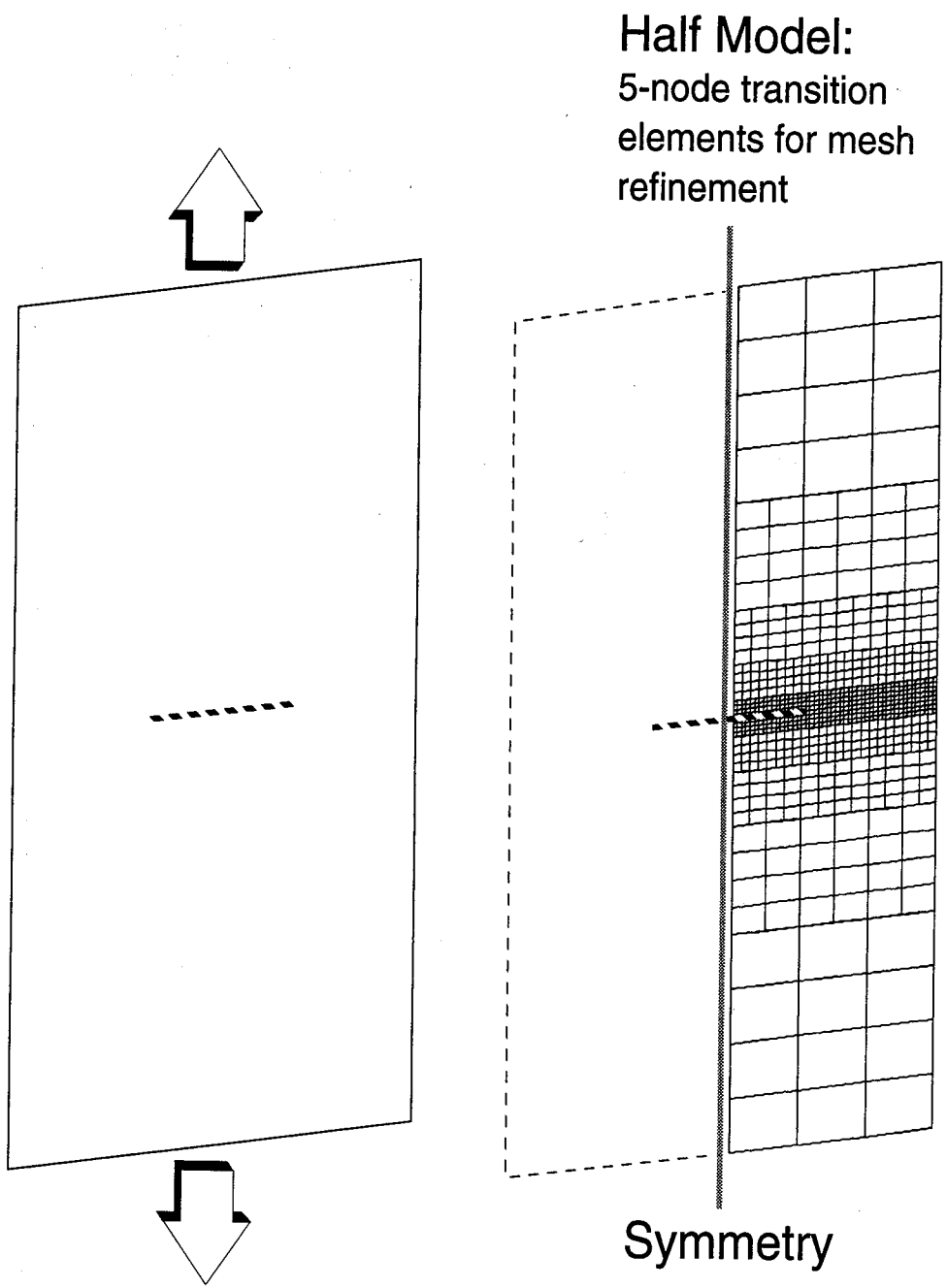

Fig. 19 Finite element model of a flat aluminum panel with a transverse center crack.

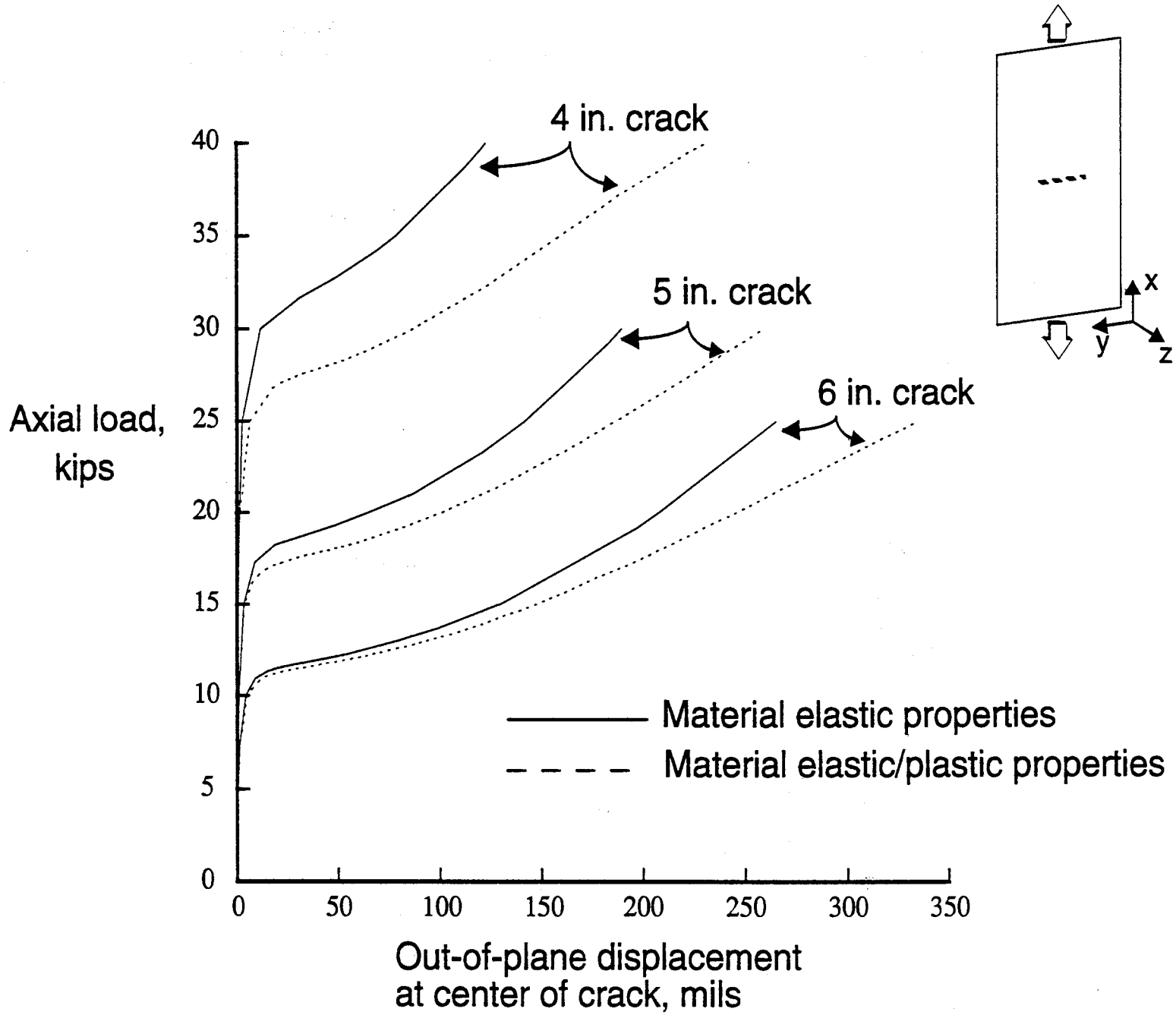

Fig. 20 Out-of-plane displacements at the crack center for tension-loaded panels with elastic and elastic-plastic material properties.

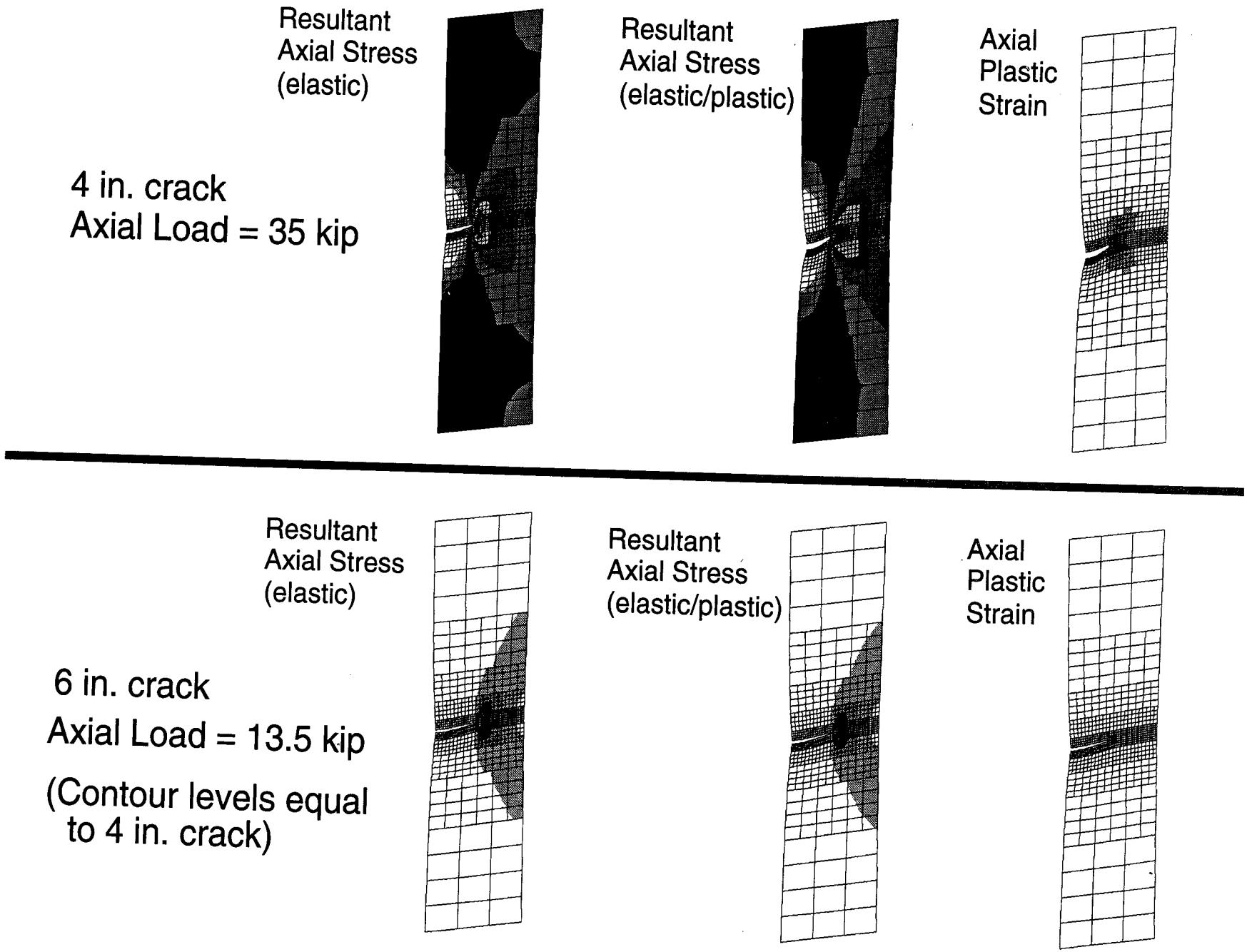

Fig. 21 Axial stress resultants and plastic strains for panels with applied tension loads that are 20 percent greater than the panel buckling loads.